

# Supporting information for In-situ X-Ray Raman spectroscopy of LiBH<sub>4</sub>

---

Piter S. Miedema<sup>1\*</sup>, Peter Ngene<sup>1</sup>, Ad M.J. van der Eerden<sup>1</sup>, Tsu-Chien Weng<sup>2</sup>, Dennis Nordlund<sup>2</sup>, Dimosthenis Sokaras<sup>2</sup>, Roberto Alonso-Mori<sup>3</sup>, Amélie Juhin<sup>1</sup>, Petra E. De Jongh<sup>1</sup> and Frank M.F. de Groot<sup>1\*</sup>

<sup>1</sup>Department of Inorganic Chemistry and Catalysis, Debye Institute for Nanomaterials Science, Utrecht University, Universiteitsweg 99, 3584 CG Utrecht, The Netherlands.

<sup>2</sup>Stanford Synchrotron Radiation Light Source, SLAC National Accelerator Laboratory, 2575 Sand Hill Road, Menlo Park, CA 94025, United States.

<sup>3</sup>Linear Coherent Light Source, SLAC National Accelerator Laboratory, 2575 Sand Hill Road, Menlo Park, CA 94025, United States

\* [f.m.f.degroot@uu.nl](mailto:f.m.f.degroot@uu.nl); [p.s.miedema@gmail.com](mailto:p.s.miedema@gmail.com)

## Table of Contents

I. EXPERIMENTAL X-RAY RAMAN SPECTRA OF Li <sub>4</sub> SiO <sub>4</sub> AND BN.....	2
II. B and Li K-edge XAS calculations: crystal structures and supercell sizes .....	3
III. B K-EDGE XAS CALCULATIONS .....	4
IV. Li K-EDGE XAS CALCULATIONS.....	6

## I. EXPERIMENTAL X-RAY RAMAN SPECTRA OF $\text{Li}_4\text{SiO}_4$ AND BN

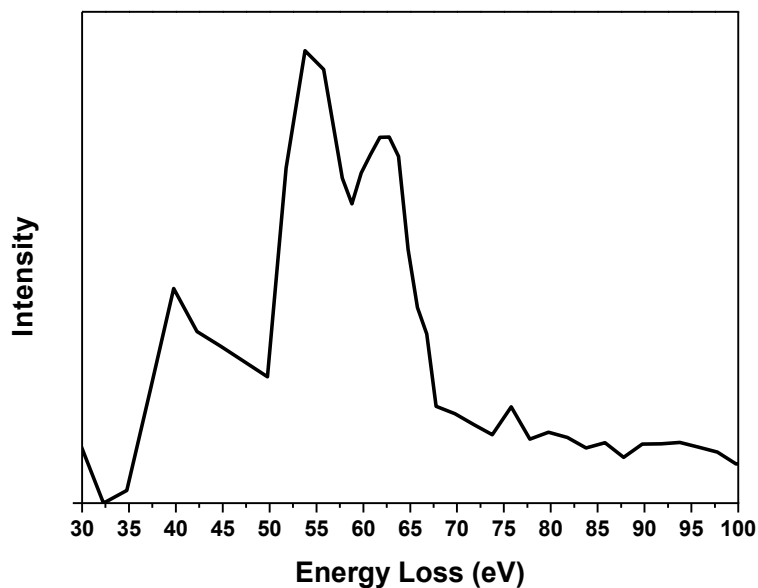


FIG. S1. Li K-edge X-Ray Raman spectrum of  $\text{Li}_4\text{SiO}_4$

FIG. S1 shows the Li K-edge XRS of  $\text{Li}_4\text{SiO}_4$ . The shape of the spectrum agrees with data from Bergmann et al.,<sup>1</sup> but the exact energy where peaks are is different. The data is noisy after background subtraction, which shows that the subtraction is a very delicate process in this case and actually in all cases of Li K-edges.

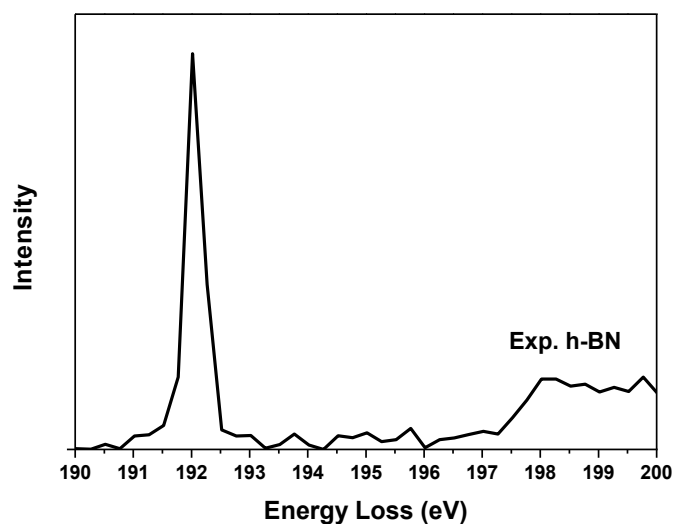


FIG. S2. B K-edge X-Ray Raman spectrum of h-BN

FIG. S2 shows the experimental B K-edge XRS of h-BN powder. The spectrum is similar to other XAS spectra of BN,<sup>2</sup> but there are some differences with other XRS<sup>3</sup> and EELS

experiments.<sup>4</sup> This difference might be ascribed to the difference in the studied samples: either single-crystal h-BN, or polycrystalline h-BN crystals or h-BN powder in this study.

## **II. B and Li K-edge XAS calculations: crystal structures and supercell sizes**

In Table 1 the investigated materials and their crystal structures are shown together with the used supercell size and the k-points for the XANES calculations with the Quantum-Espresso package are shown.

**Table 1.** Crystal structures and the supercell sizes and k-point grid used in the self-consistent field (scf) calculations.

Structure	Structure information	Supercell size	K-points (scf)	Reference
LiB	Pnma	2x4x2	4x4x4	J.K. Kang et al. <sup>5</sup>
LiBH	Pnma	2x4x2	4x4x4	J.K. Kang et al. <sup>5</sup>
LiBH <sub>4</sub>	Pnma	2x2x2	3x3x3	J.K. Kang et al. <sup>5</sup>
LiBH <sub>4</sub> HT	P6 <sub>3</sub> mc	2x2x2	4x4x4	J.-Ph. Soulié et al. <sup>6</sup> , data for LiBH <sub>4</sub> at 408K
BN	P 6 <sub>3</sub> /mmc	4x4x2	4x4x4	R.S. Pease <sup>7</sup>
Li (metal)	Fm3m	2x2x2	4x4x4	www-MINCRYST(2011) <sup>8</sup> , card nr. 2605
B (tetra)	P4(2)/nnm	1x1x2	5x5x5	www-MINCRYST(2011) <sup>8</sup> , card nr. 593
B (hexa)	R3(-)m	2x2x1	4x4x4	www-MINCRYST(2011) <sup>8</sup> , card nr. 594
LiH	Fm3m	4x4x4 /5x5x5	1x1x1	Ref. <sup>9</sup>
Li <sub>2</sub> B <sub>12</sub> H <sub>12</sub>	Pa-3	1x1x1	4x4x4	J.-. Her et al. <sup>10</sup>
B <sub>2</sub> O <sub>3</sub>	P3 <sub>1</sub> 21-c <sup>2</sup> a	2x2x1	8x8x8	H. Effenberger et al. <sup>11</sup>

### III. B K-EDGE XAS CALCULATIONS

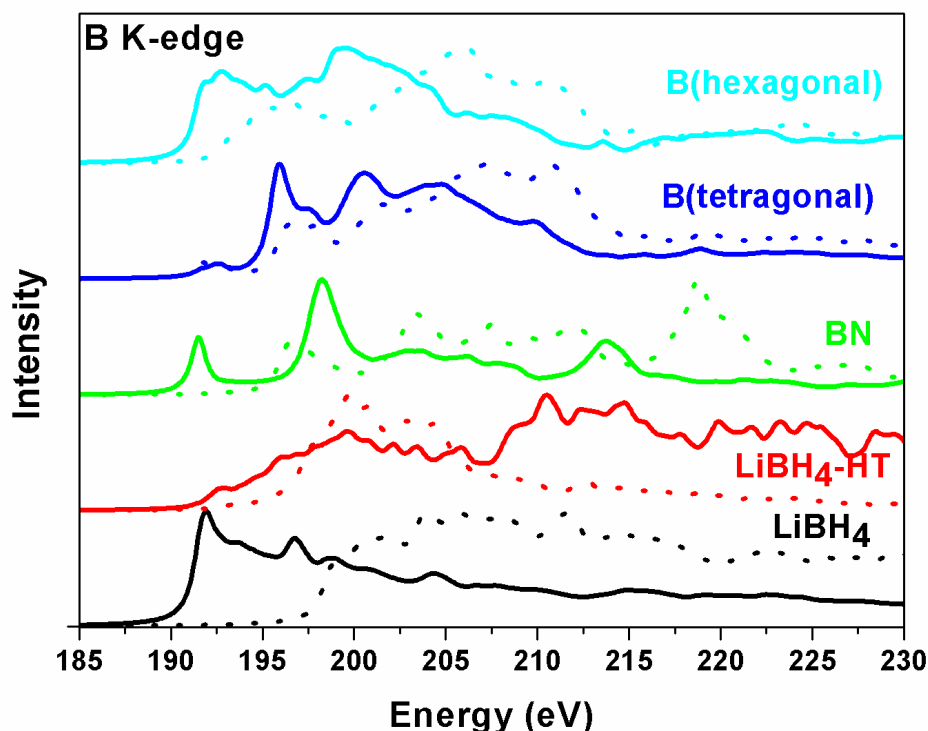


FIG. S3. B K-edge XAS calculations for LiBH<sub>4</sub> (black lines), LiBH<sub>4</sub>-HT (red lines), BN (green lines) and B(hexagonal) (blue lines) and B(tetragonal) (light blue lines). Solid lines represent the calculations with full core-hole and the dotted lines are the calculations without core-hole.

FIG. S3 shows the B K-edge XAS calculations for LiBH<sub>4</sub> (as in Fig. 2B in main text), for a high temperature phase of LiBH<sub>4</sub>, BN, and tetragonal and hexagonal boron. It is clear that the high temperature phase is not visible in our experimental data in the main text (Fig. 3A and Fig. 3C). The only possible material that may be present in our experiment is tetragonal boron. However, the rest of the peaks is not visible in the experimental XRS.

Focusing on the BN calculations, there is agreement with our experimental spectrum FIG. S2, but the calculated peak at 197 eV is not that intense and sharp as in the XRS. However this peak is observed in other experimental spectra, so this might be due to higher crystallinity in our calculations compared to the XRS of h-BN powder.

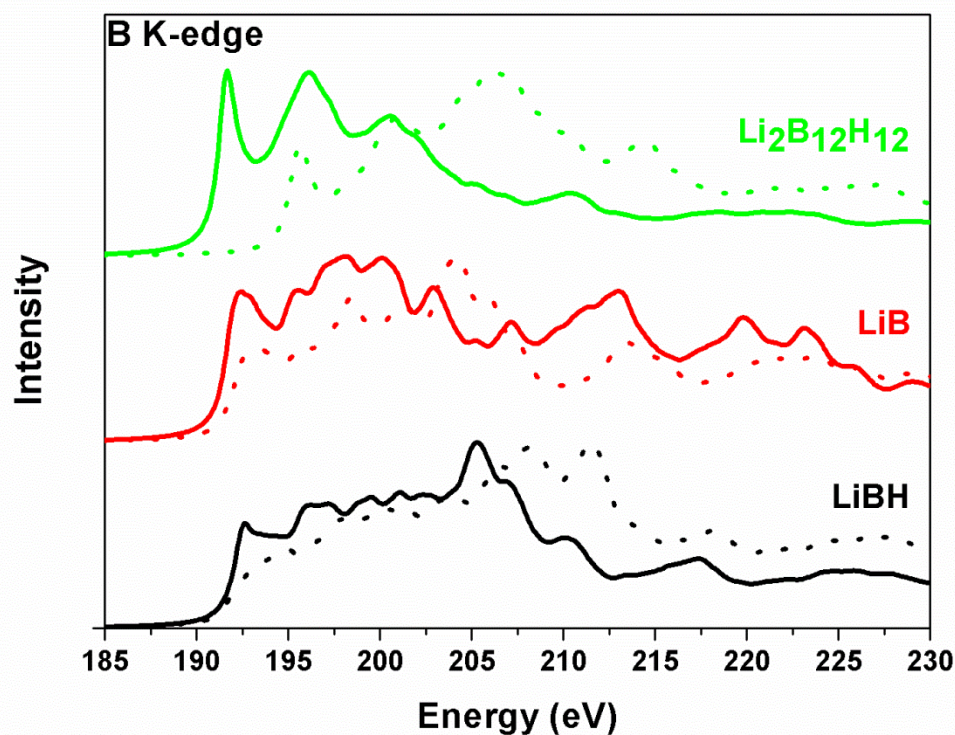


FIG. S4. B K-edge XAS calculations for LiBH (black lines), LiB (red lines) and Li<sub>2</sub>B<sub>12</sub>H<sub>12</sub> (green lines) Solid lines represent the calculations with full core-hole and the dotted lines are the calculations without core-hole.

FIG. S4 shows the B K-edge XAS calculations for the possible intermediate compounds LiBH, LiB and Li<sub>2</sub>B<sub>12</sub>H<sub>12</sub>. At first glance it might be possible that there is Li<sub>2</sub>B<sub>12</sub>H<sub>12</sub> in our experiment, since a peak close to 194 eV is visible in the solid green line calculation. However in our experimental spectra at higher temperatures shown in the main text (FIG. 3C) the second peak of the calculated Li<sub>2</sub>B<sub>12</sub>H<sub>12</sub> just at about 196 eV is not visible, which leads to the conclusion that no Li<sub>2</sub>B<sub>12</sub>H<sub>12</sub> is present in the experiments shown in the main text.

#### IV. Li K-EDGE XAS CALCULATIONS

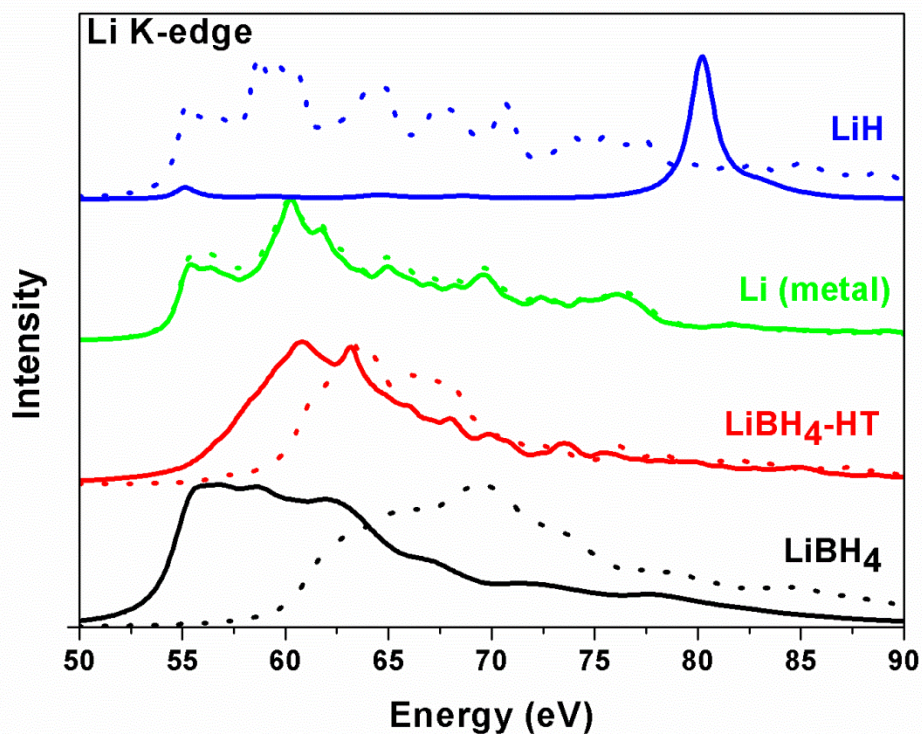


FIG. S5. Li K-edge XAS calculations for LiBH<sub>4</sub> (black lines), LiBH<sub>4</sub>-HT (red lines), Li(metal) (green lines) and LiH (blue lines). Solid lines represent the calculations with half core-hole and the dotted lines are the calculations without core-hole.

FIG. S5 shows the Li K-edge XAS calculations for LiBH<sub>4</sub>, for a high temperature phase of LiBH<sub>4</sub>, Li (metal) and LiH. Since there are clear differences between all the spectra, we can conclude that the experimental XRS of bulk LiBH<sub>4</sub> powder at higher temperatures in the main text (Fig. 3B) only accounts for LiBH<sub>4</sub>.



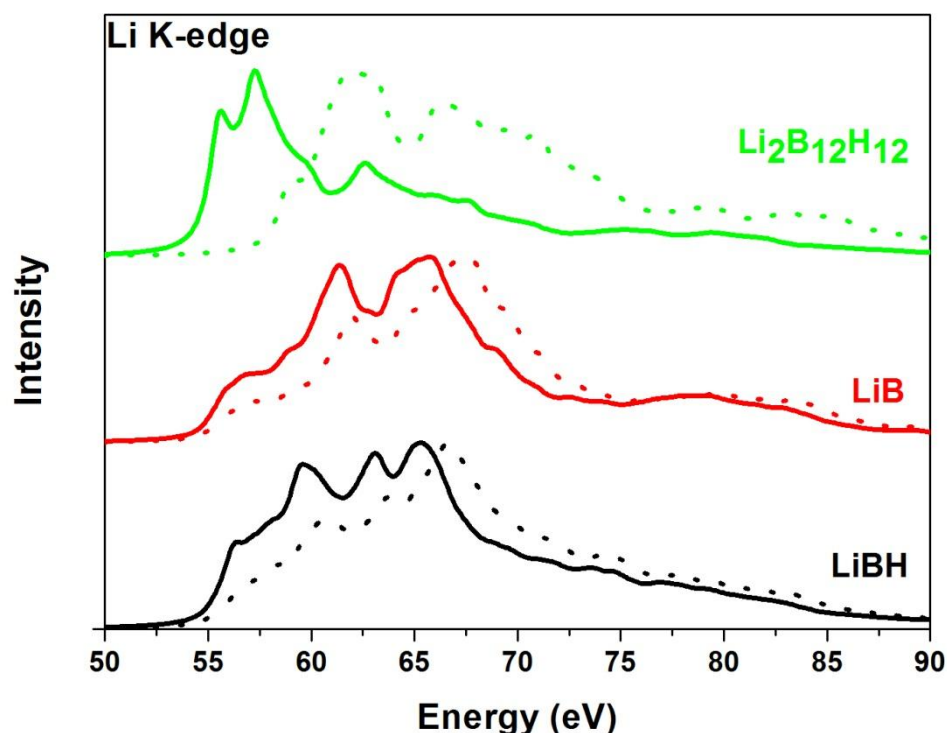


FIG. S6. Li K-edge XAS calculations for  $\text{LiBH}$  (black lines),  $\text{LiB}$  (red lines),  $\text{Li}_2\text{B}_{12}\text{H}_{12}$  (green lines). Solid lines represent the calculations with half core-hole and the dotted lines are the calculations without core-hole.

FIG. S6 shows the Li K-edge XAS calculations for the possible intermediate compounds  $\text{LiBH}$ ,  $\text{LiB}$  and  $\text{Li}_2\text{B}_{12}\text{H}_{12}$ . In the experimental Li K-edge XRS at elevated temperatures shown in the main text for 25wt%  $\text{LiBH}_4/\text{C}$  (Fig 5D), there is a possibility that the patterns of  $\text{LiBH}$ ,  $\text{LiB}$  and  $\text{Li}_2\text{B}_{12}\text{H}_{12}$  are present in the experimental XRS, but then the B K-edge calculated patterns should also have been visible in the experimental XRS spectra of Fig 5C. These combined arguments lead to the conclusion that Fig. 5D shows no intermediate products, but either the intercalated Li ( $\text{LiC}_6$ ) or  $\text{LiO}_x\text{H}_y$  formation.

## References

- (1) Bergmann, U.; Glatzel, P.; Cramer, S. P. Bulk-sensitive XAS characterization of light elements: From X-ray Raman scattering to X-ray Raman spectroscopy. *Microchem. J.* **2002**, *71*, 221-230.
- (2) MacNaughton, J. B.; Moewes, A.; Wilks, R. G.; Zhou, X. T.; Sham, T. K.; Taniguchi, T.; Watanabe, K.; Chan, C. Y.; Zhang, W. J.; Bello, I.; Lee, S. T.; Hofsäss, H. Electronic structure of boron nitride single crystals and films. *Phys. Rev. B Condens. Matter Mater. Phys.* **2005**, *72*, 1-8.
- (3) Meng, Y.; Mao, H. -.; Eng, P. J.; Trainor, T. P.; Newville, M.; Hu, M. Y.; Kao, C.; Shu, J.; Hausermann, D.; Hemley, R. J. The formation of  $\text{sp}^3$  bonding in compressed BN. *Nat. Mater.* **2004**, *3*, 111-114.

- (4) Arenal, R.; de la Peña, F.; Stéphan, O.; Walls, M.; Tencé, M.; Loiseau, A.; Colliex, C. Extending the analysis of EELS spectrum-imaging data, from elemental to bond mapping in complex nanostructures. *Ultramicroscopy* **2008**, *109*, 32-38.
- (5) Kang, J. K.; Kim, S. Y.; Han, Y. S.; Muller, R. P.; Goddard III, W. A. A candidate LiBH<sub>4</sub> for hydrogen storage: Crystal structures and reaction mechanisms of intermediate phases. *Appl. Phys. Lett.* **2005**, *87*, 1-3.
- (6) Soulié, J. -.; Renaudin, G.; Erný, R.; Yvon, K. Lithium boro-hydride LiBH<sub>4</sub>: I. Crystal structure. *J Alloys Compd* **2002**, *346*, 200-205.
- (7) Pease, R. S. An X-ray study of boron nitride. *Acta Crystallogr.* **1952**, *5*, 356-361.
- (8) WWW-MINCRYST (2011). Crystallographic and Crystallochemical Database for minerals and their structural analogues. <http://database.iem.ac.ru/mincryst>.
- (9) <http://www.oxmat.co.uk/Crysdata/lih.htm>.
- (10) Her, J. -.; Yousufuddin, M.; Zhou, W.; Jalisatgi, S. S.; Kulleck, J. G.; Zan, J. A.; Hwang, S. -.; Bowman Jr., R. C.; Udovic, T. J. Crystal structure of Li<sub>2</sub>B<sub>12</sub>H<sub>12</sub>: A possible intermediate species in the decomposition of LiBH<sub>4</sub>. *Inorg. Chem.* **2008**, *47*, 9757-9759.
- (11) Effenberger, H.; Lengauer, C. L.; Parthe, E. Trigonal B<sub>2</sub>O<sub>3</sub> with higher space-group symmetry: Results of a reevaluation. *Monatsh. Chem.* **2001**, *132*, 1515-1517.